

# Nanoscale Mapping of Built-in Potential in GaAs p–n Junction Using Light-Modulated Scanning Tunneling Microscopy

Shoji YOSHIDA, Yuya KANITANI, Ryuji OSHIMA, Yoshitaka OKADA, Osamu TAKEUCHI, and Hidemi SHIGEKAWA

*Institute of Applied Physics, CREST-JST, University of Tsukuba, Tsukuba, Ibaraki 305-8573, Japan*

(Received February 7, 2008; revised March 21, 2008; accepted April 17, 2008; published online July 18, 2008)

Surface photovoltage (SPV) was visualized over the interface of a GaAs p–n junction using light modulated scanning tunneling spectroscopy. Spatially resolved SPV includes information about the built-in potential of the p–n junction as well as the photo-induced relaxation of tip-induced band bending. These two components were separately evaluated, and mapping of the built-in potential was accomplished on the nanoscale. [DOI: 10.1143/JJAP.47.6117]

KEYWORDS: scanning tunneling microscopy, surface photovoltage, semiconductor, GaAs, p–n junction

## 1. Introduction

With the development of nanoscale science and technology, we are now facing the limits of fundamental issues. Through the miniaturization of semiconductor devices down to less than 50 nm, for example, fluctuation in the distribution of atomic defects or dopant materials on the nanoscale now directly affects the macroscopic functions.<sup>1)</sup> Fluctuation of component materials or irregularity of ordering at a hetero-semiconductor interface also results in the variation of the local potential.<sup>2)</sup> To achieve fine control of these basic elements, it is desired to establish techniques that enable us to characterize the physical properties of materials and devices in relation to the nanoscale structures.

Scanning probe microscopy (SPM) is one of the most prominent candidates for this purpose. Various techniques based on SPM have thus far been developed.<sup>3–13)</sup> Among them, light modulated scanning tunneling spectroscopy (LM-STs) enables us to evaluate the local potential in semiconductor devices on the nanoscale, through the measurement of surface photovoltage (SPV).<sup>5,6)</sup> In scanning tunneling microscopy (STM) on a semiconductor sample, band bending is induced in the surface region by the leakage of the electric field produced by the bias voltage applied between the STM tip and the sample;<sup>5,6,12)</sup> this phenomenon is called tip induced band bending (TIBB). When the sample surface below the STM tip is photo-illuminated, carriers are excited and redistributed to reduce TIBB,<sup>12–14)</sup> where the shift of the current–voltage ( $I$ – $V$ ) curves between dark and photoilluminated conditions provides SPV. Using LM-STM, SPV can be visualized on the nanoscale.

Since TIBB depends on the local carrier density, information about the dopant profile and excess minority carriers injected into a p–n junction can be obtained by LM-STM.<sup>5)</sup> For a p–n junction, the intrinsic band bending produced by the equalization of the Fermi level on both sides, built-in potential, which is an important factor in hetero-semiconductor devices, is also modified by photo-illumination, contributing to the SPV detected by LM-STM. Therefore, built-in potential can be probed by LM-STM. However, since TIBB is also included in SPV, how to distinguish the two components is the essential point. In this study, we demonstrate a method for probing the built-in potential, free from the effect of TIBB, and visualize it on the nanoscale.

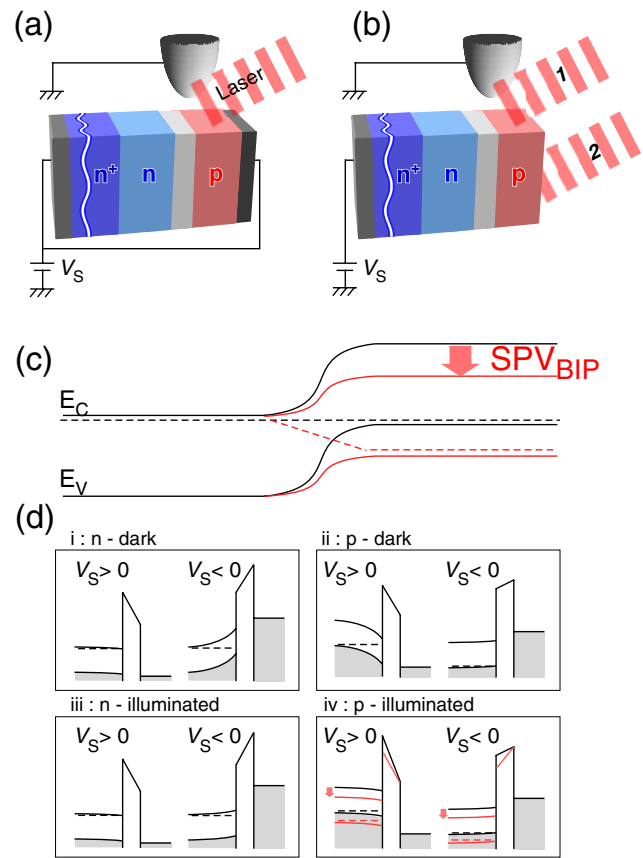


Fig. 1. (Color online) (a, b) Schematic illustrations of experimental setup for three different conditions. (c) Potential of p–n junction.  $E_C$ ,  $E_V$ , and  $SPV_{BIP}$  represent the conduction band minimum, valence band maximum and surface photovoltage due to the reduction of built-in potential, respectively. (d) I–D band structures of metal–insulator–semiconductor (MIS) configuration of STM measurement. i, ii: Dark condition. iii, iv: Under photoillumination. The change in the built-in potential [SPV in (c)] observed for the open-circuit setup is also shown in iv by red lines.

## 2. Experimental Methods

Experiments were carried out under UHV ( $<1 \times 10^{-8}$  Pa) conditions at room temperature. A p–n junction was prepared by growing n-type (Si-doped,  $2.0 \times 10^{18} \text{ cm}^{-3}$ , 500 nm) and p-type (Be-doped,  $2.0 \times 10^{18} \text{ cm}^{-3}$ , 500 nm) GaAs layers on an n-GaAs(001) substrate. Both ends of the sample were connected to electrodes [Fig. 1(a)], or the end of the p-type side was opened [Fig. 1(b)], depending on the

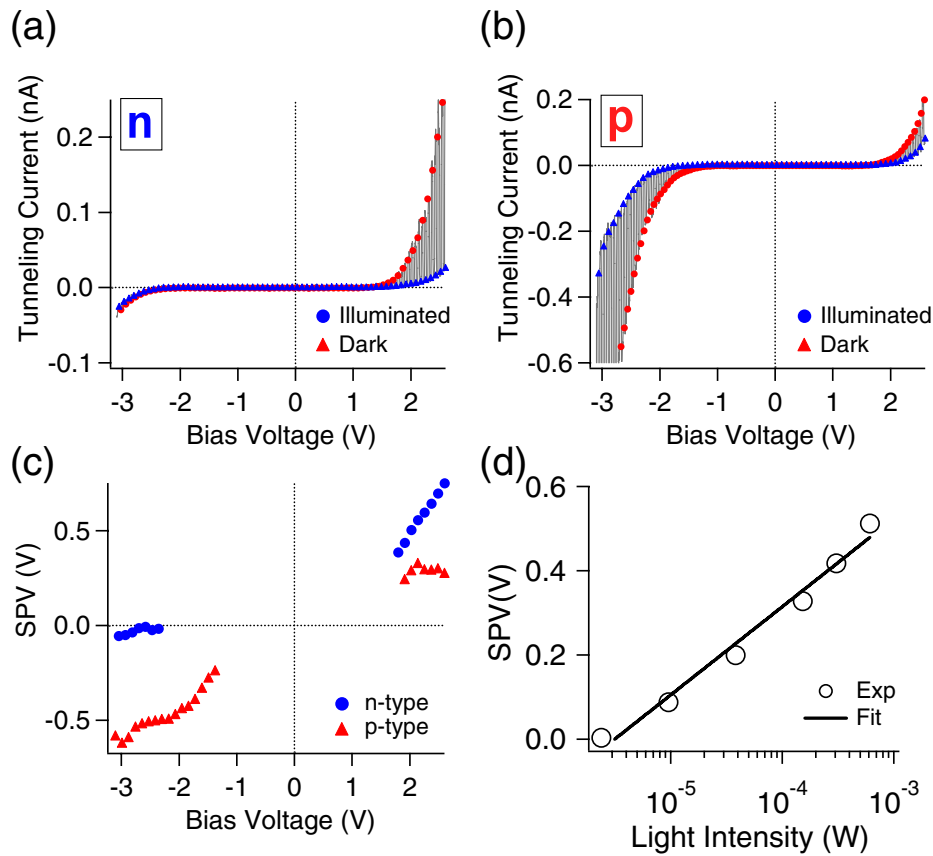


Fig. 2. (Color online) (a, b)  $I$ - $V$  curves obtained for the condition shown in Fig. 1(b)-1. (c) Sample-bias voltage-dependent SPV. Blue and red lines are derived from the  $I$ - $V$  curves in (a) and (b). (d) Light intensity dependence of SPV.

experiment. Mechanically chopped illumination from a laser diode (635 nm, 100 Hz), 60° off-normal to the surface, was focused onto the sample with a spot diameter of 0.02 mm. In the case of the open circuit [Fig. 1(b)], light-spot position 1 or 2 was adopted depending on the experiment. An electrochemically etched tungsten tip was used.

### 3. Results and Discussion

Figure 1(c) shows a schematic illustration of the potential in a p-n junction. Band bending due to the charge transfer to equalize the Fermi energy on both sides of n- and p-type region corresponds to built-in potential. If both electrodes are closed [Fig. 1(a)], SPV produced by the reduction of TIBB,  $SPV_{TIBB}$ , is large (small) at positive (negative) sample bias voltages for the n-type (p-type) region, due to the positional relation between the conduction (valence) band edge and the Fermi energy [Fig. 1(d), black lines]. However, when the end of the p-type side is open [Fig. 1(b)], large SPV is expected to appear at positive bias voltages for the p-type region, due to the reduction of the built-in potential under photoillumination, surface photovoltage  $SPV_{BIP}$  [Figs. 1(c) and 1(d)-iv, red lines].

Figures 2(a) and 2(b) show typical  $I$ - $V$  curves obtained for n- and p-type regions. For a positive-sample-bias-voltage condition shown in Fig. 2(a), tunneling current oscillates due to the change in  $SPV_{TIBB}$  caused by the chopped-laser illumination, and the two virtual  $I$ - $V$  curves, which correspond to those under dark (blue dotted line) and illuminated (red solid line) conditions, can be simultaneously obtained. The SPV spectrum [blue dots in Fig. 2(c)] is

obtained by calculating the lateral shift of the two  $I$ - $V$  curves with respect to the bias voltage for the  $I$ - $V$  curve under the dark condition. The central part of the spectrum with the tunneling current below 3 pA is missing due to the difficulty in calculating the shift of the two  $I$ - $V$  curves in that region.  $SPV_{TIBB}$  is small for the negative sample bias region as expected.

In contrast, in the case of the p-type region [Fig. 2(b)], tunneling current oscillates for both positive and negative bias voltages, and a notable point is that the SPV observed in the positive sample-bias voltage region is bias-independent,  $\sim 0.3$  V, as shown by the red dots in Fig. 2(c). Since  $SPV_{TIBB}$  is bias-dependent and appears only in the p-type layer for negative sample-bias voltage, this SPV observed for the p-type layer is attributed to the reduction of the built-in potential under photoillumination,  $SPV_{BIP}$ .

From the theory of superband-gap illumination, SPV has a logarithmic dependence on the light intensity  $I$  as  $SPV = C \ln(I/I_0)$ ,<sup>14,15</sup> where  $I_0$  is an arbitrary light intensity used for normalization, and  $C$  is a constant needed for unit conversion. Figure 2(d) shows the relationship between  $I$  and SPV ( $= SPV_{BIP}$ ) obtained by averaging the values measured over the p-type area ( $300 \times 400 \text{ nm}^2$ ) far from the interface of the p-n junction with a positive sample bias voltage (+2.5 V). The agreement between the theory and the experimental results indicates that our method can quantitatively provide  $SPV_{BIP}$  in a semiconductor device regardless of the TIBB effect.

As has been seen, with the open-circuit condition shown in Fig. 1(b)-1, we confirmed that there are two components

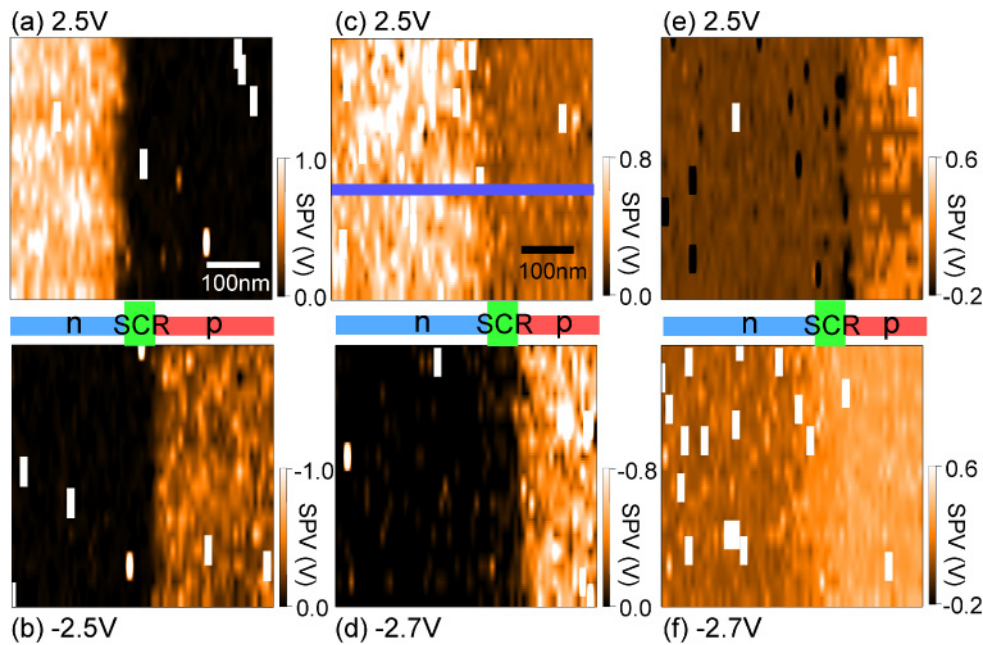


Fig. 3. (Color online) SPV-mapping images obtained under the three different conditions (a–b, c–d, e–f) corresponding to those in Fig. 1(a), Fig. 1(b)-1, and Fig. 1(b)-2, respectively.

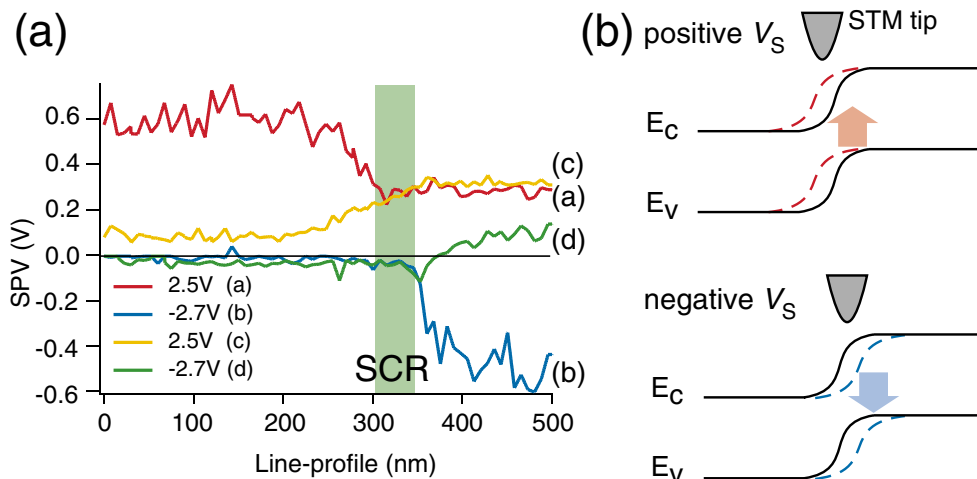


Fig. 4. (Color online) (a) Cross sections of mapping images in Figs. 3(c) to 3(f), along the blue line in Fig. 3(c). (b) Apparent changes in the potential of p–n junction with positive (upper) and negative (lower) bias voltages.

in SPV, namely,  $SPV_{TIBB}$  and  $SPV_{BIP}$ , and succeeded in distinguishing  $SPV_{BIP}$  from  $SPV_{TIBB}$ . Next, we show the results of  $SPV_{BIP}$  mapping over the p–n junction. If the laser spot is focused below the STM tip [Fig. 1(b)-1], both  $SPV_{TIBB}$  and  $SPV_{BIP}$  are included in SPV, which is unprofitable for the mapping of SPV. One way to be free from the effect of TIBB is to use the fact that TIBB is a local effect appearing just below the STM tip. Namely, we can remove the  $SPV_{TIBB}$  component by illuminating only the p-type layer, away from the tunnel junction [Fig. 1(b)-2].

Figures 3(a) to 3(f) show SPV-mapping images obtained under the conditions shown in Figs. 1(a), 1(b)-1, and 1(b)-2. Since  $SPV_{TIBB}$  is dominant with the closed-circuit condition [Figs. 1(a)], a large SPV (=  $SPV_{TIBB}$ ) is observed over the n-type (p-type) region for positive (negative) sample bias voltages, as explained before using the 1D-band structures in Fig. 1(d). The intermediate region (marked by the green

rectangle) where SPV is small under both bias polarities is the space-charge region (SCR) produced in a p–n junction interface due to charge transfer. In SCR, the concentration of photo-generated carriers rapidly decreases due to the drift caused by the lateral electric field existing in this region. Therefore, photogenerated carriers do not relax the TIBB, and  $SPV_{TIBB}$  is suppressed in this region. As reported in our previous paper, these SPV images reflect local doping profiles.<sup>5)</sup>

In contrast,  $SPV_{BIP}$  is included for the open-circuit condition [Fig. 1(b)], where the end of the n-type region is grounded. When the sample surface below the STM tip is photoilluminated [Fig. 1(b)-1], both effects appear in SPV (=  $SPV_{TIBB}$  +  $SPV_{BIP}$ ). Therefore, SPV is observed even in the p-type region at +2.5 V. The cross sections of Figs. 3(c) and 3(d), along the blue line in Fig. 3(c), are shown in Fig. 4(a).

Furthermore, when the light spot is moved away from the STM tunneling junction to the end of the p-type region [Fig. 1(b)-2], the effect of  $SPV_{TIBB}$  is eliminated, and only the SPV induced by the change in built-in potential ( $SPV \sim SPV_{BIP}$ ) can be visualized.

In fact, the SPVs obtained at +2.5 and -2.7 V for the p-type region are close to each other. The small SPV ( $\sim 0.1$  V) observed here for the n-type region at +2.5 V [yellow line (c) in Fig. 4(a)] is due to the existence of  $SPV_{TIBB}$  caused by the weak illumination leaking into the tunnel junction. In the p-type region, the SPV under negative bias voltages [green line (d)] is lower than that obtained for positive bias voltages [yellow line (c)], which is caused by the  $SPV_{TIBB}$  ( $\sim -0.2$  V) induced under the negative bias-voltage condition.

Although  $SPV_{BIP}$  should increase from the SCR region,  $SPV_{BIP}$  appears even in the n-type region under positive bias voltages as shown by the yellow line (c). To understand this result, let us see how TIBB affects the potential of the p-n junction. Figure 4(b) shows a one-dimensional (1-D) band diagram of the p-n junction with the effect of TIBB under positive (top) and negative (bottom) bias voltages. Under positive bias voltage, the STM tip locally induces upward band bending, resulting in the apparent positional shift of the junction interface toward the n-type region.<sup>16)</sup> The opposite directional effect occurs under negative sample bias voltage [Fig. 4(b) bottom]: the interface position apparently shifts toward the p-type region, [green line (d) in Fig. 4(a)]. The observed gradual slope of  $SPV_{BIP}$  extending over 50 nm (yellow line) reflects the size of TIBB at this bias voltage.

#### 4. Conclusions

In conclusion, we demonstrated a method of nanoscale-mapping of the built-in potential of a GaAs p-n junction using LM-STs. The spatially resolved SPV obtained by LM-STM includes information about the built-in potential of the p-n junction as well as the photo-induced relaxation of tip induced band bending. These two components were separately evaluated, and mapping of the built-in potential

was accomplished on the nanoscale. These results indicate the potential of LM-STs as a promising method of probing the nanoscale characteristics of advanced semiconductor devices of the future.

#### Acknowledgements

This work was supported in part by a Grant-in-Aid for Scientific Research from the Ministry of Education, Culture, Sports, Science, and Technology of Japan. We thank Ms. Rie Yamashita, in our group at the University of Tsukuba, for her help in preparing this paper.

- 1) B. Cheng, S. Roy, G. Roy, F. Adamu-Lema, and A. Asenov: *Solid-State Electron.* **49** (2005) 740.
- 2) N. D. Jäger, K. Urban, E. R. Weber, and Ph. Ebert: *Appl. Phys. Lett.* **82** (2003) 2700.
- 3) K. Kimura, K. Kobayashi, H. Yamada, K. Matsushige, and K. Usuda: *J. Vac. Sci. Technol. B* **24** (2006) 1371.
- 4) D. Ban, E. H. Sargent, St. J. Dixon-Warren, I. Calder, A. J. SpringThorpe, R. Dworschak, G. Este, and J. K. White: *Appl. Phys. Lett.* **81** (2002) 5057.
- 5) S. Yoshida, Y. Kanitani, R. Oshima, Y. Okada, O. Takeuchi, and H. Shigekawa: *Phys. Rev. Lett.* **98** (2007) 26802.
- 6) O. Takeuchi, S. Yoshida, and H. Shigekawa: *Appl. Phys. Lett.* **84** (2004) 3645.
- 7) Y. Terada, M. Aoyama, H. Kondo, A. Taninaka, O. Takeuchi, and H. Shigekawa: *Nanotechnology* **18** (2007) 44028.
- 8) H. Shigekawa, O. Takeuchi, and M. Aoyama: *Sci. Technol. Adv. Mater.* **6** (2005) 582.
- 9) H. Shigekawa, S. Yoshida, O. Takeuchi, M. Aoyama, Y. Terada, H. Kondo, and H. Oigawa: *Thin Solid Films* **516** (2008) 2348.
- 10) S. Yoshida, J. Kikuchi, Y. Kanitani, O. Takeuchi, H. Oigawa, and H. Shigekawa: *e-J. Surf. Sci. Nanotechnol.* **4** (2006) 192.
- 11) S. Yoshida, Y. Kanitani, O. Takeuchi, and H. Shigekawa: *Appl. Phys. Lett.* **92** (2008) 102105.
- 12) M. McEllistrem, G. Haase, D. Chen, and R. J. Hamers: *Phys. Rev. Lett.* **70** (1993) 2471.
- 13) S. Grafstrom: *J. Appl. Phys.* **91** (2002) 1717.
- 14) L. Kronik and Y. Shapira: *Surf. Sci. Rep.* **37** (1999) 1.
- 15) R. Shikler, N. Fried, T. Meoded, and Y. Rosenwaks: *Phys. Rev. B* **61** (2000) 11041.
- 16) N. D. Jäger, M. Marso, M. Salmeron, E. R. Weber, K. Urban, and Ph. Ebert: *Phys. Rev. B* **67** (2003) 165307.